Official journal of the JHL 2689-9620
www.light-am.com

Article Open Access

Efficient synthesis of vitamin D_3 in a 3D ultraviolet photochemical microreactor fabricated using an ultrafast laser

Aodong Zhang[1,2,3], Jian Xu[1,2,3,*], Lingling Xia[1], Ming Hu[1,*], Yunpeng Song[2,3], Miao Wu[3] and Ya Cheng[1,2,3,4,*]

Abstract

Large-scale, high-precision, and high-transparency microchannels hold great potential for developing high-performance continuous-flow photochemical reactions. We demonstrated ultrafast laser-enabled fabrication of three-dimensional microchannel reactors in ultraviolet (UV) grade fused silica which exhibit high transparency under the illumination of UV light sources of wavelengths well below 300 nm with excellent mixing efficiency. With the fabricated glass microchannel reactors, we demonstrated continuous-flow photochemical synthesis of vitamin D_3 with UV LED array light sources.

Keywords: Ultrafast laser microfabrication, Fused silica microchannels, UV photochemical reactors, Continuous-flow synthesis, Vitamin D_3

Introduction

Vitamin D_3 (VD3) has important applications in biomedicine and clinical therapy, consequently creating a substantial market demand for its large-scale and high-purity production[1–5]. VD3 can be photochemically generated in the bodies of animals and humans from 7-dehydrocholesterol (7-DHC) initiated by proper ultraviolet (UV) light irradiation (particularly within the spectral range of 275–300 nm). Currently, industrial synthesis of VD3 predominantly relies on photochemical reactions, wherein 7-DHC is irradiated by UV light to yield pre-vitamin D_3, thermally isomerizing into VD3. However, traditional photochemical synthesis conducted in batch photoreactors suffers from low photon utilization efficiencies, limiting the 7-DHC conversions. The yield of VD3 is often less than 20%, giving rise to low production efficiency, high production cost, and unwanted byproducts and isomers caused by long-term irradiations. The emergence of microfluidic technology and the integration of continuous-flow chemical reactions into photochemical synthesis have ushered in new prospects for fine chemicals and pharmaceutical synthesis[6–13]. Although continuous-flow chemical synthesis has prominent advantages for drug and drug intermediate production, current research and application of continuous-flow photochemical microreactions primarily utilize visible light (400–700 nm) and medium-to-long-wavelength UV light (300–400 nm) as irradiation sources[9,12,13]. To date, UV-irradiation continuous-flow chemical synthesis of VD3 faces several critical limitations on microreactor materials and UV light

Correspondence: Jian Xu (jxu@phy.ecnu.edu.cn) or Ming Hu (mhu@phy.ecnu.edu.cn) or Ya Cheng (ya.cheng@siom.ac.cn)
[1]Engineering Research Center for Nanophotonics and Advanced Instrument, School of Physics and Electronic Science, East China Normal University, Shanghai 200241, China
[2]State Key Laboratory of Precision Spectroscopy, School of Physics and Electronic Science, East China Normal University, Shanghai 200241, China
Full list of author information is available at the end of the article.

sources. Regarding the microreactor materials, conventional transparent UV polymer-based microreactors, such as fluorinated ethylene propylene (FEP) tubes[14,15], inevitably degrade under the long-term operation of UV light irradiation and high temperatures. Moreover, current commercially available glass microchannel reactors (made of borosilicate glass)[11,12,16,17] exhibit poor UV light transmission rates in the short-wavelength UV spectrum, hindering high-efficiency photon utilization for UV photochemical synthesis. Fused silica glass, renowned for its superior UV transparency ranging from 200 nm to 400 nm, represents an ideal microreactor material for such reactions. Moreover, due to its excellent chemical inertness, the fused silica reactor can be easily cleaned and reusable. However, the fabrication of micro-reaction chips in fused silica is challenging due to the difficulties in microfabrication and high-performance bonding of fused silica glass[18]. The existing fused silica glass microchannel reactors primarily comprise glass capillaries of uniform circular cross-sections, which are not ideal for achieving efficient fluid manipulation and high photon irradiation efficiency. Furthermore, most UV continuous-flow photochemical microreactors employ medium- and high-pressure mercury lamps as UV light sources, which greatly consume power[2,3,5,19]. In some cases, polymer tubes or fused silica capillaries are coiled around these high-power lamps. For long-term operation, effective thermal management of these reactors is needed due to the inevitable heat generated by these lamps, impeding the scale-up production of conventional UV photochemical synthesis methods. This necessitates stringent demands on the temperature control system throughout the reactor. To overcome the difficulties, the development of a new UV-light-enabled continuous-flow photochemical fused silica microchannel reactor system is highly desirable.

Due to the feature of nonlinear multiphoton absorption associated with the extremely high peak intensity, an ultrafast laser provides a powerful tool for spatially selective modification and micro/nanostructuring in transparent dielectrics such as glass, which holds great potential for developing numerous novel applications in photonics and microfluidics[20–22]. Ultrafast laser-assisted etching based on a two-step procedure (i.e., ultrafast laser irradiation followed by chemical etching[23–25]) has been recognized as one of the most representative methods for 3D glass microchannel fabrication. Compared with conventional lithographic methods, ultrafast laser-assisted etching of glass microchannels offers many distinct advantages, such as bonding-free fabrication, almost arbitrary configurations, high-precision features, and multiple functionalities. However, although many remarkable advances have been made in the past two decades, simultaneous fabrication of 3D large-scale and high-precision glass channels remains a challenge due to the inherent limitation of laser-induced etching selectivity[26–28]. For instance, bonding-free fabrication of a uniform microchannel with a length of tens of centimeters is technically difficult, hindering many practical applications of this powerful technology. To address this issue, recently we proposed a hybrid laser microfabrication approach based on a combination of ultrafast laser microfabrication of fused silica assisted by carbon dioxide (CO_2) laser processing for sealing the extra-access holes left behind the ultrafast laser microfabrication[29,30]. Herein, we demonstrated further progress in the manufacture of 3D large-scale UV photochemical fused silica microchannel reactors and the efficient synthesis of VD3 in the reactors. Ultrafast laser direct writing is first employed to create 3D embedded micropatterns in UV grade fused silica including the patterns of 3D microchannels and a string of extra-access holes between the channels and glass surfaces. The distribution of extra-access holes is optimized to improve the subsequent etching homogeneity of the laser-modified structures. After chemical etching, the holes are sealed by defocused CO_2 laser irradiation to form closed microchannel structures with a few inlets and outlets for introducing chemical reagents into the microchannels and extracting the products out of the microreactor. With the manufactured glass microchannel reactor, complex micro-reaction conditions, such as high temperature (~160 ℃), high pressure (~2.0 MPa), and high-efficiency UV irradiation, can be simultaneously loaded for long-term operation. Furthermore, we demonstrated continuous-flow photochemical synthesis of VD3 with UV LED array light sources in a single step.

Results and discussion

Manufacture of a 3D large-scale fused silica microchannel reactor

The manufacture of a 3D large-scale fused silica microchannel reactor is based on the hybrid laser microfabrication, which combines the merits of ultrafast laser-assisted etching, extra-access holes for enhancing the etching, and CO_2 laser-induced in-situ melting of glass surface for hole sealing. As illustrated in Fig. 1a, the manufacturing flow for a 3D large-scale fused silica microchannel structure consists of three main procedures: (i) ultrafast laser direct writing of 3D microchannels comprised of 3D micro-mixing units and a string of vertical extra-access holes evenly distributed along the channel; (ii) selective chemical etching for removing the

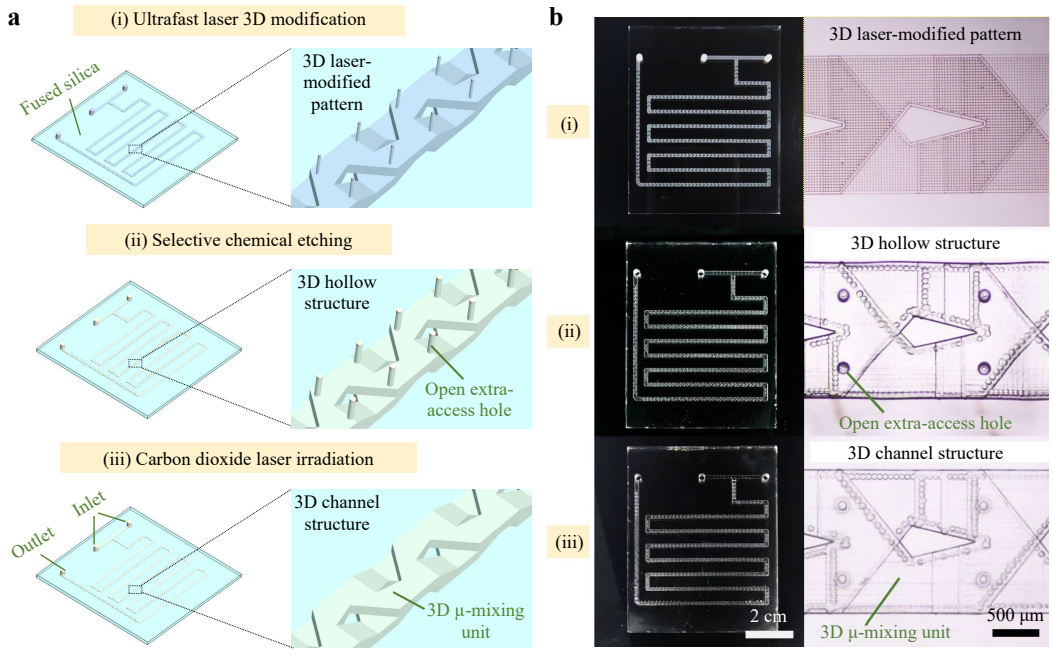

Fig. 1 a Schematic of the manufacturing procedure for a 3D large-scale fused silica microchannel reactor, which consists of three main steps: (i) Ultrafast laser 3D modification; (ii) Selective chemical etching; (iii) Carbon dioxide laser irradiation. The right panel in each step presents a close-up view of the processed structure indicated by a dashed rectangle on the left panel. **b** Photographs of a processed fused silica glass plate with a size of 78 mm × 63 mm × 3 mm (left panel) and top-view optical micrographs of 3D glass microstructures (right panel) in the plate at each step in **a**. The width, height, and length of the whole microchannel in **b** were approximately 1.53, 0.25, and 475 mm, respectively.

laser-modified micropatterns to obtain a hollow microchannel with a string of through holes reaching the glass surface; (iii) CO_2 laser irradiation for sealing the holes to form a closed large-scale microchannel structure with a few necessary inlets and outlets. First, an ultrafast laser beam was focused through an objective lens inside the fused silica to generate modified micropatterns. The micropatterns included an embedded large-scale microchannel with 3D micro-mixing units and a string of vertical extra-access holes along the channel in fused silica. Compared to a straight microchannel, a glass channel with 3D micromixing units based on the baker's transformation provides enhanced mixing performance at the microscale space, as shown in Figure S1[27,30]. After laser modification, the sample was immersed in the etching solution under the ultrasonic water bath to selectively remove all laser-modified materials. The introduction of extra-access holes was adopted to break the inherent limitations of the selectivity of conventional ultrafast laser-assisted etching and achieve the homogenous fabrication of large-scale glass microchannels, enabling greatly enhanced etching performance of the microchannels[29–31]. Finally, the etched holes were sealed by defocused CO_2 laser irradiation on the glass surface to form the final large-scale fused silica microchannel structure. The defocused CO_2 laser irradiation provides a more spatially controllable sealing of those holes as compared with direct laser irradiation due to the improved intensity distribution for in-situ melting on the glass surface[29–31]. The spot size of the defocused CO_2 laser beam was larger than the dimension of the holes on the glass surface for rapid and controllable melting of the surrounding area of the holes (see Figure S2). With optimized irradiation parameters, the holes could be sealed to form sealing layers with thicknesses of several hundred microns, which gives rise to the high-pressure resistance of the manufactured microchannel structures up to several MPa. To demonstrate the manufacturing capabilities of the proposed method, a 3D large-scale microchannel structure was processed inside a fused silica glass plate with a size of 78 mm × 63 mm × 3 mm shown in Fig. 1b. The left and right panels in Fig. 1b show photographs of the processed glass plate and top-view optical micrographs of embedded 3D glass microstructures in the plate at each fabrication step illustrated in Fig. 1a, respectively. The manufactured microchannel's width, height, and length were approximately 1.53, 0.25, and 475 mm, respectively.

For high-performance UV photochemical synthesis, the substrate material of the microreactor is of vital importance for high-efficiency utilization of UV photon energies. Transmittance curves of commercial borosilicate glass (the

most commonly used materials for continuous-flow microchannel reactors) and fused silica with different thicknesses were measured and compared at multiple wavelengths ranging from 200 nm to 320 nm to identify the superior advantages of fused silica for UV photochemical microreactors. As shown in the left panel of Fig. 2, for borosilicate glass samples with different thicknesses, there was strong absorption of UV photon energies. Moreover, the transmittance of the glass severely decreased as the thickness increased. For instance, as presented in the right panel of Fig. 2, when the thickness of borosilicate glass increased from 1 mm to 3 mm, the corresponding transmittance value reduced from ~61.5% to ~14.4% at 275 nm. In contrast, the fused silica glass sample with different thicknesses exhibited high transmission rates at all the wavelengths in the range of 200–320 nm. Especially, as shown in the right panel of Fig. 2, the transmittance values of all fused silica samples were maintained to be above 90% at the wavelengths of 255, 275, 290, and 310 nm regardless of thickness. Therefore, the adoption of fused silica as reactor material is highly preferable to achieve a high photon utilization rate for UV photochemical synthesis.

Construction of a continuous-flow UV photochemical synthesis system

After the manufacture of the fused silica microchannel reactor, we built a continuous-flow UV photochemical synthesis system as illustrated in Fig. 3a. This system comprises a plunger pump, a fused silica microchannel reactor, a UV LED array light source, a surface heater, an external back-pressure valve, and a cooling box. The inlet and outlet of the fused silica microchannel reactor were connected to the plunger pump and a back-pressure valve using polytetrafluoroethylene (PTFE) tubes, respectively. The bottom surface (i.e., the surface of the microreactor without the sealed access holes) of the microchannel reactor was attached to the surface heater while the top surface was attached to the UV LED light source. The entire device was of a sandwich layout in the order of LED-light source, fused silica microreactor, and surface heater. The interior temperature (available in the range of 25–350 °C) and pressure (available in the range of 0–3.5 MPa) of the microchannel reactor were controlled by the surface heater and back-pressure valve, respectively. The solutions of raw materials in a glass container were first pumped by the plunger pump into the microchannel reactor at the controlled back pressures and temperatures. Then, the on-chip photochemical reaction was performed under UV light irradiation. After flowing through the back-pressure value, the high-temperature reactants were cooled down to room temperature or even lower in the cooling box (the cooling medium could be liquid nitrogen, dry ice, and ice water, among others) before entering the final collection containers. The UV-LED array light source is composed of an array of UV-LED lamp beads at predesignated wavelengths. The irradiation power of the surface light source is determined by the power of a single lamp bead, the number of lamp beads per unit area, and the wiring density. Fig. 3b presents a typical photo of a continuous-flow UV photochemical synthesis system in a fume hood. As compared with conventional UV photochemical systems based on batch-production methods, our home-built system provides superior performance for thermal management and UV light utilization of microreactor, which holds great potential for high-throughput and large-scale production.

On-chip UV photochemical synthesis of Vitamin D_3

In the UV photochemical microreaction system, as

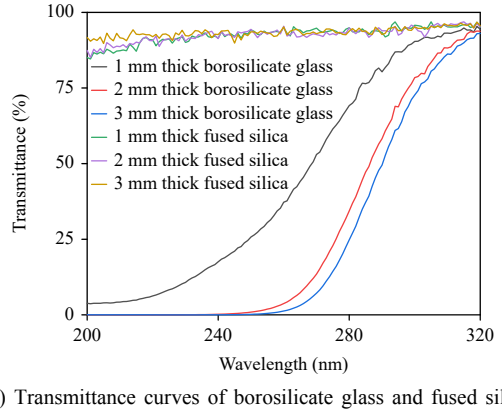

Wavelength (nm)	Transmittance (%)					
	Borosilicate glass			Fused silica		
	1 mm thick	2 mm thick	3 mm thick	1 mm thick	2 mm thick	3 mm thick
255	30.5	1.9	0.5	93.1	92.8	93.2
275	61.5	22.9	14.4	94.1	93.0	94.1
290	80.4	58.2	49.5	93.4	93.9	92.7
310	93.1	88.2	86.3	95.2	95.4	95.7

Fig. 2 (Left) Transmittance curves of borosilicate glass and fused silica with different thicknesses at the wavelength from 200 nm to 320 nm; (Right) Comparison of the transmittances of borosilicate glass and fused silica with different thicknesses at the wavelengths of 255, 275, 290, and 310 nm.

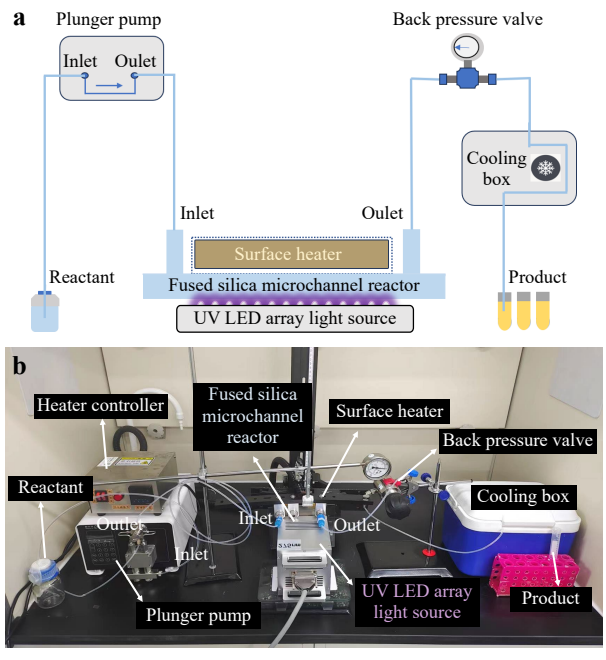

Fig. 3 a Schematic and **b** photograph of continuous-flow UV photochemical synthesis system based on the fabricated fused silica microchannel reactor. The fused silica microchannel reactor was vertically placed between a surface heater and the UV LED array light source.

shown in Fig. 3b, the synthesis of VD3 includes the following procedures. First, the precursor solution was prepared by dissolving the 7-dehydrocholesterol (7-DHC) in *tert*-butyl methyl ether (t-BME)[5]. Second, the solution was pumped into the glass microchannel reactor with an interior pressure of 2.0 MPa and a temperature of 160 ℃. After stabilizing the pressure and temperature of the microchannel reactor, the UV LED light irradiation was initiated for on-chip continuous-flow photochemical synthesis. Then, the reactant solutions were cooled down and collected for chemical analysis and characterization, such as UV-vis absorption spectrum and high-performance liquid chromatography (HPLC). Herein, the influence of different continuous-flow photochemical synthesis conditions such as UV irradiation wavelengths and flow rates of reactant solutions on the synthesis performance of VD3 was systematically investigated.

Fig. 4a shows the typical absorbance spectra of the synthesized products under the irradiation of UV LED array light sources (optical power: ~3.8 W) at different wavelengths (255, 275, 290, and 310 nm) with a flow rate of 0.2 mL/min (residence time: ~2.6 min). Two characteristic peaks in the absorption spectrum of a standard VD3 sample are observed at 213 and 264 nm (see Figure S3). These two characteristic peaks at 213 and 264 nm are used to determine the formation of VD3. However, the absorption at 264 nm is close to one of the characteristic absorption peaks of the standard 7-DHC sample (see Figure S4). Therefore, using the intensity of the characteristic absorption peak at 213 nm for characterization is more precise. From the variation of the intensity of the characteristic absorption peak at 213 nm in Fig. 4a, the corresponding UV irradiation wavelength with the maximum absorption intensity of the characteristic absorption peak of VD3 at 213 nm was 275 nm, which was of higher yield as compared with the UV irradiation sources at other wavelengths. The average values of the intensities of the characteristic absorption peaks at 213 nm were calculated and plotted in Fig. 4b to quantitatively determine the influence of the irradiation wavelength on photochemical synthesis. At the same irradiation powers of the LED array light sources, the 275 nm light source provides the maximum synthesized intensity among the different UV irradiation wavelengths (255, 275, 290, and 310 nm). HPLC was employed to separate the synthesized products and detect the VD3 molecules for further confirming the successful synthesis of VD3. The emergence of the absorption at the retention time of ~6.9 min correlates to the formation of VD3 (see Figures S5 and S6). In contrast, the products obtained without UV irradiation only showed a small absorption at the retention time of ~7.0 min, suggesting that the UV-induced photoreaction is responsible for the formation of VD3 (see Figures S6 and S7). Compared with conventional VD3 continuous-flow photochemical reactions and photothermal stepwise reactions[2–5], the VD3 yield and conversion rate of 7-DHC through one-step synthesis reported in this study were approximately 36% and 88% by identifying the peak area percentages of VD3 and 7-DHC based on HPLC analysis results[3–5,32,33] (see Figure S6), respectively. The corresponding selectivity (i.e., the ratio of the yield of VD3 and the conversion rate of 7-DHC) was ~41%. In Fig. 4c, besides the difference in UV irradiation, both the synthesized products were obtained under the same conditions (flow rate: 0.2 ml/min, temperature: 160 ℃, pressure: 2 MPa). According to the HPLC analysis results, the yield of VD3 was ~3% under high-temperature and high-pressure conditions when there was no UV irradiation, as shown in Figure S7. In contrast, when the UV irradiation (275 nm) was performed, the yield of VD3 increased to approximately 36% at the same conditions. In this case, regarding the concentration of the reactant (~21 g/L) and the yield of VD3 (~36%), the estimated productivity of a single photochemical microchannel reactor (0.2 ml/min, 275 nm irradiation) per year is ~0.795 kg. The high yield may be ascribed to the effective

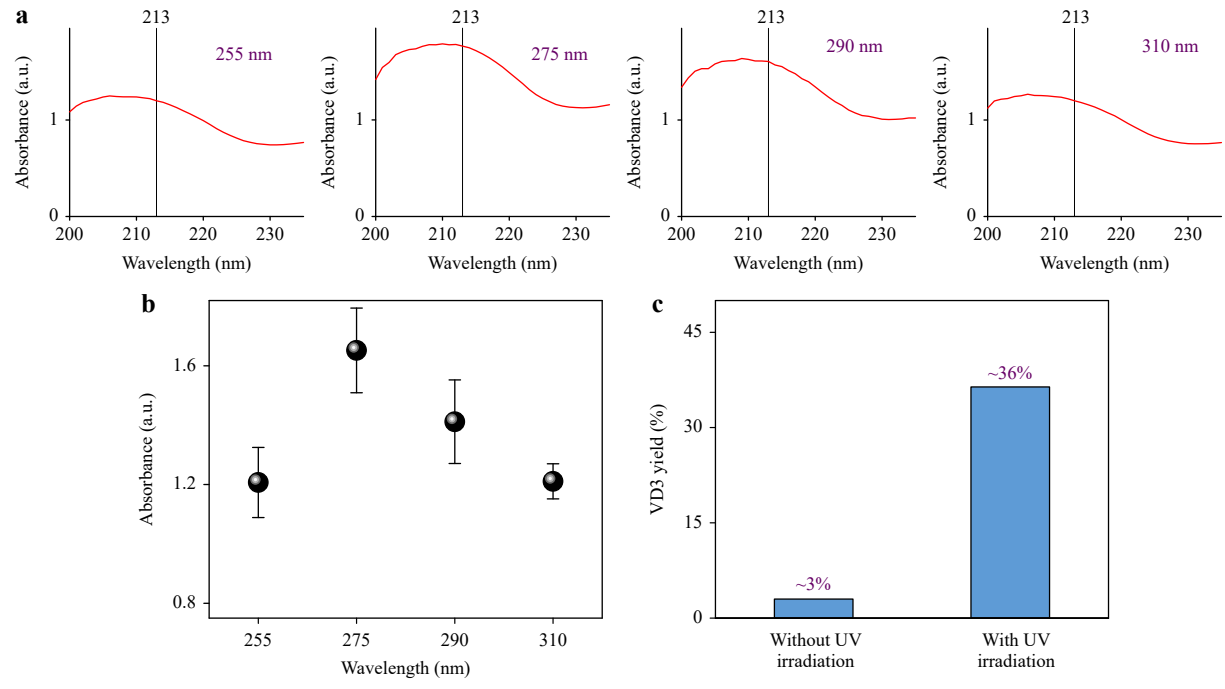

Fig. 4 a Absorbance spectra of the synthesized products under the irradiation of UV LED array light sources at different UV irradiation wavelengths (255, 275, 290, and 310 nm) with a flow rate of 0.2 mL/min. **b** The intensity of the characteristic absorption peak at 213 nm of the products versus UV irradiation wavelengths in **a**. **c** VD3 yield in the synthesized products without and with UV irradiation based on HPLC analysis results.

manipulation of reactant solutions in the UV-illuminated region in the fabricated microchannel reactor with 3D micromixing units[27,30], high UV-photon-absorption efficiency of the reaction liquids in the reactor, and synergetic application of the high-pressure and high-temperature conditions[5].

Fig. 5a shows the absorption spectra of the products that were obtained under 275 nm LED array irradiation (optical power: ~4.2 W) at the different flow rates of reactant solutions (0.5, 1.0, 1.5, and 2.0 mL/min). The increase in the flow rate causes the decrease in the residence time of the on-chip photochemical reaction, decreasing the intensity of the characteristic peak at 213 nm, as shown in Fig. 5b. The average intensity of the absorption peaks of the products at 213 nm decreased to 0.8 when the flow rate was raised to 2 mL/min. Since the residence time is related to the total liquid inventory of the microchannel reactor, further improvement of the throughput and performance of UV photochemical synthesis can be achieved by increasing the volume size of the microreactor while maintaining the high mixing and heat transfer efficiencies, which will be the focus of our future investigation.

In summary, a one-step continuous-flow UV photochemical synthesis of VD3 is demonstrated in the 3D large-scale fused silica microchannel reactor fabricated using an ultrafast laser. Compared with conventional UV photochemical microreactors, the proposed technique has the following advantages. First, the fabricated 3D microchannel reactor allows simultaneous operation of high-efficiency UV irradiation, high pressure, and high temperature for efficiency improvement in the continuous flow synthesis, enabling a single-step and efficient synthesis of VD3. The yield of synthesized VD3 and the corresponding selectivity reached approximately 36% and 41%, respectively. Second, compared with traditional continuous-flow UV photochemical synthesis using high-pressure mercury lamps as radiation sources, the photochemical synthesis based on UV LED array-assisted irradiation provides a more efficient and stable route for UV photon energy utilization and long-term temperature control[34–36]. Accordingly, the thermal management during UV photochemical synthesis can be effectively controlled, which will be beneficial for further scale-up and mass production. Finally, compared with conventional visible photochemical synthesis heavily relying on expensive catalysts, the fused silica microreactor is expected to develop a series of catalyst-free UV photochemical synthesis strategies due to its unique capability of operating under high-energy UV photon irradiation.

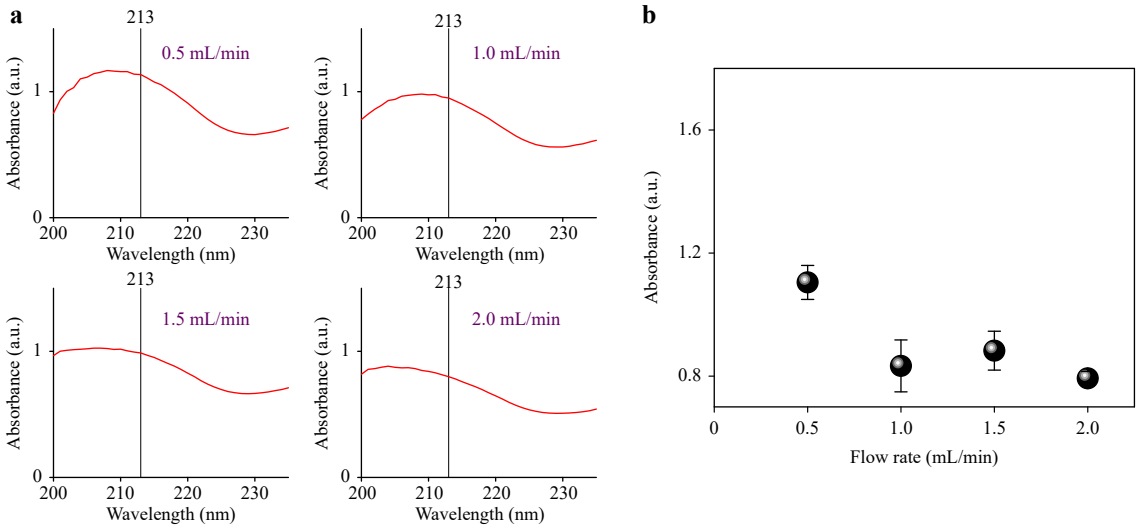

Fig. 5 a Absorbance spectra of the synthesized products using different flow rates (0.5, 1.0, 1.5, and 2.0 mL/min) of reactants under the 275 nm LED array irradiation. **b** Intensity of the characteristic absorption peak at 213 nm of the products versus flow rate of the reactant solution in **a**.

Materials and Methods

Fabrication of fused silica microchannel reactors

For 3D laser modification, an ultrafast laser amplifier system (Pharos 20 W, Light Conversion, Lithuania) with a central wavelength of 1030 nm, a tunable pulse width of 0.27–10 ps, a repetition rate of 250 kHz, and a maximum pulse energy of 0.4 mJ was employed. The fused silica glass samples (JGS1) were placed on a 3D motorized stage (Coretech 3D X-Y-Z stage, Coretech, China) and irradiated by the focused laser beam through an infrared objective lens with a numerical aperture of 0.26 (M Plan Apo NIR 10X, Mitutoyo, Japan). The spot sizes of the ultrafast laser beam before and after focusing were approximately 4.5 mm and 4.8 μm, respectively. The laser writing speed, line-by-line, and layer-by-layer writing spacing were 100 mm/s, 30 μm, and 50 μm, respectively. For chemical etching, the laser-processed glass samples were immersed in a 10 M KOH etching solution at 95 ℃ under an ultrasonic bath until all modified regions were removed. For CO_2 laser irradiation, a defocused CO_2 laser beam (FSTi100SWC, Synrad, USA) with a repetition rate of 20 kHz was used to seal the extra-access holes. The CO_2 laser beam was focused through a ZnSe lens (LA7028-E3, Thorlabs, USA) with a focal length of 159 mm and induced in-situ sealing on the openings of the extra-access holes on the glass surface one by one with the translation of a 2D motorized stage (OneXY-500-500-AS-CMS1, Coretech, China). The average power of the CO_2 laser beam before the ZnSe lens, the defocusing distance of the CO_2 laser beam, and the spot size of the defocused laser beam on the glass surface were approximately 46.1 W, 32 mm, and 3.6 mm, respectively. The laser irradiation time for sealing a single extra-access hole was 10 s. In a manufactured photochemical microchannel reactor with a size of 155 mm × 125 mm × 2 mm, there are two inlets and one outlet with an identical diameter of 3.1 mm, an embedded 3D microchannel, and 742 extra-access holes. The microchannel's width, height, and length were approximately 3.08, 0.37, and 790 mm, respectively. The diameters and heights of the extra-access holes were approximately 245 and 800 μm, respectively. The processing time for ultrafast laser direct writing, chemical etching, and CO_2 laser irradiation were 10, 48, and 2.1 h, respectively.

On-chip continuous-flow UV photochemical synthesis

For on-chip photochemical synthesis, a precursor solution with a concentration of 21 mg/mL was prepared by dissolving 7-DHC in t-TBE. The 7-DHC solution was driven by a plunger pump (DPS-100, Oushisheng, China) into the inlet of the chip, and the chip with a size of 155 mm × 125 mm × 2 mm was attached to a UV LED light source and a surface heater, forming a triple-layer sandwich structure such that the UV light irradiation and the reaction temperature of the channel reactor could be simultaneously controlled for photo- and thermo-reactions. The illumination areas of all UV LED light sources were 100 mm × 100 mm. The liquid holdups of the fabricated microchannel reactor and UV-illuminated microchannel in the reactor were estimated as 0.66 and 0.53 mL, respectively. Before the UV irradiation, the temperature of

the microchannel reactor was calibrated using the heater and an infrared thermometer. During the on-chip continuous-flow synthesis, the temperature of 160 ℃ and the pressure of 2 MPa in the microchannel reactor were kept constant. The collected products were characterized by a UV absorption spectrometer (UV-2600, Shimadzu, Japan) and a high-performance liquid chromatography (Agilent 1100, Agilent Technologies, USA).

Acknowledgements
This work was supported by the National Natural Science Foundation of China (Grant Nos. 12174107, 61991444, 11933005, 12192251, and 12334014), National Key R&D Program of China (Grant No. 2019YFA0705000), Science and Technology Commission of Shanghai Municipality (Grant No. 21DZ1101500), Shanghai Municipal Science and Technology Major Project, and Fundamental Research Funds for the Central Universities.

Author details
[1]Engineering Research Center for Nanophotonics and Advanced Instrument, School of Physics and Electronic Science, East China Normal University, Shanghai 200241, China. [2]State Key Laboratory of Precision Spectroscopy, School of Physics and Electronic Science, East China Normal University, Shanghai 200241, China. [3]XXL —The Extreme Optoelectromechanics Laboratory, School of Physics and Electronic Science, East China Normal University, Shanghai 200241, China. [4]State Key Laboratory of High Field Laser Physics, Shanghai Institute of Optics and Fine Mechanics, Chinese Academy of Sciences, Shanghai 201800, China

Author contributions
Y. Cheng supervised the research work. J. Xu, M. Hu, and Y. Cheng conceived the experiments. A. Zhang, J. Xu, L. Xia, M. Hu, Y. Song, and M. Wu carried out the experiments. A. Zhang, J. Xu, and M. Hu contributed to the data analysis. All authors participated and contributed to the writing of the manuscript.

Conflict of interest
The authors declare no competing interests.

Supplementary information is available for this paper at https://doi.org/10.37188/lam.2024.010.

Received: 12 September 2023 Revised: 27 December 2023 Accepted: 17 January 2024
Accepted article preview online: 18 January 2024
Published online: 16 March 2024

References

1. Galkin, O. N. & Terenetskaya, I. P. 'Vitamin D' biodosimeter: basic characteristics and potential applications. *Journal of Photochemistry and Photobiology B. Biology* **53**, 12-19 (1999).
2. Fuse, S. et al. Continuous-flow synthesis of vitamin D_3. *Chemical Communications* **46**, 8722-8724 (2010).
3. Fuse, S. et al. Continuous-flow synthesis of activated vitamin D_3 and its analogues. *Organic & Biomolecular Chemistry* **10**, 5205-5211 (2012).
4. Escribà-Gelonch, M. et al. Laser-mediated photo-high-p, T intensification of vitamin D_3 synthesis in continuous flow. *ChemPhotoChem* **2**, 922-930 (2018).
5. Escribà-Gelonch, M., Noël, T. & Hessel, V. Microflow high-p, T intensification of vitamin D_3 synthesis using an ultraviolet lamp. *Organic Process Research & Development* **22**, 147-155 (2018).
6. Oelgemöeller, M. Highlights of photochemical reactions in microflow reactors. *Chemical Engineering & Technology* **35**, 1144-1152 (2012).
7. Su, Y. H. et al. Photochemical transformations accelerated in continuous-flow reactors: basic concepts and applications. *Chemistry - A European Journal* **20**, 10562-10589 (2014).
8. Cambié, D. et al. Applications of continuous-flow photochemistry in organic synthesis, material science, and water treatment. *Chemical Reviews* **116**, 10276-10341 (2016).
9. Buglioni, L. et al. Technological innovations in photochemistry for organic synthesis: flow chemistry, high-throughput experimentation, scale-up, and photoelectrochemistry. *Chemical Reviews* **122**, 2752-2906 (2022).
10. Tomarelli, E. et al. Merging continuous flow technology, photochemistry and biocatalysis to streamline steroid synthesis. *Advanced Synthesis & Catalysis* **365**, 4024-4048 (2023).
11. Rehm, T. H. Reactor technology concepts for flow photochemistry. *ChemPhotoChem* **4**, 235-254 (2020).
12. Zhang, M. X. & Roth, P. Flow photochemistry - from microreactors to large-scale processing. *Current Opinion in Chemical Engineering* **39**, 100897 (2023).
13. Xie, J. L. & Zhao, D. Y. Continuous-flow photochemistry: an expanding horizon of sustainable technology. *Chinese Chemical Letters* **31**, 2395-2400 (2020).
14. Niu, W. H. et al. Photochemical microfluidic synthesis of vitamin D_3 by improved light sources with photoluminescent substrates. *Chinese Journal of Chemical Engineering* **29**, 204-211 (2021).
15. Bachollet, S. et al. Microflow photochemistry: UVC-induced [2 + 2]-photoadditions to furanone in a microcapillary reactor. *Beilstein Journal of Organic Chemistry* **9**, 2015-2021 (2013).
16. Steiner, A. et al. Multikilogram per hour continuous photochemical benzylic brominations applying a smart dimensioning scale-up strategy. *Organic Process Research & Development* **24**, 2208-2216 (2020).
17. Steiner, A. et al. *N*-Chloroamines as substrates for metal-free photochemical atom-transfer radical addition reactions in continuous flow. *Reaction Chemistry & Engineering* **6**, 2434-2441 (2021).
18. Domínguez, M. I. et al. Current scenario and prospects in manufacture strategies for glass, quartz, polymers and metallic microreactors: a comprehensive review. *Chemical Engineering Research and Design* **171**, 13-35 (2021).
19. Elliott, L. D. et al. A small-footprint, high-capacity flow reactor for UV photochemical synthesis on the kilogram scale. *Organic Process Research & Development* **20**, 1806-1811 (2016).
20. Sugioka, K. & Cheng, Y. Ultrafast lasers-reliable tools for advanced materials processing. *Light:Science & Applications* **3**, e149 (2014).
21. Sugioka, K. et al. Femtosecond laser 3D micromachining: a powerful tool for the fabrication of microfluidic, optofluidic, and electrofluidic devices based on glass. *Lab on a Chip* **14**, 3447-3458 (2014).
22. Piacentini, S. et al. Advanced photonic and optofluidic devices fabricated in glass via femtosecond laser micromachining [Invited]. *Optical Materials Express* **12**, 3930-3945 (2022).
23. Bellouard, Y. et al. Fabrication of high-aspect ratio, micro-fluidic channels and tunnels using femtosecond laser pulses and chemical etching. *Optics Express* **12**, 2120-2129 (2004).
24. Kiyama, S. et al. Examination of etching agent and etching mechanism on femtosecond laser microfabrication of channels inside vitreous silica substrates. *The Journal of Physical Chemistry C* **113**, 11560-11566 (2009).
25. Gottmann, J. et al. Selective laser-induced etching of 3D precision

quartz glass components for microfluidic applications - up-scaling of complexity and speed. *Micromachines* **8**, 110 (2017).
26. Cheng, Y. Internal laser writing of high-aspect-ratio microfluidic structures in silicate glasses for lab-on-a-chip applications. *Micromachines* **8**, 59 (2017).
27. Qi, J. et al. A microfluidic mixer of high throughput fabricated in glass using femtosecond laser micromachining combined with glass bonding. *Micromachines* **11**, 213 (2020).
28. Li, X. L. et al. Polarization-insensitive space-selective etching in fused silica induced by picosecond laser irradiation. *Applied Surface Science* **485**, 188-193 (2019).
29. Lin, Z. J. et al. Freeform microfluidic networks encapsulated in laser-printed 3D macroscale glass objects. *Advanced Materials Technologies* **5**, 1900989 (2020).
30. Zhang, A. D. et al. Three-dimensional large-scale fused silica microfluidic chips enabled by hybrid laser microfabrication for continuous-flow UV photochemical synthesis. *Micromachines* **13**, 543 (2022).
31. Yu, J. P. et al. Low-loss optofluidic waveguides in fused silica enabled by spatially shaped femtosecond laser assisted etching combined with carbon dioxide laser irradiation. *Optics & Laser Technology* **158**, 108889 (2023).
32. Ma, K. et al. Purity determination and uncertainty evaluation of theophylline by mass balance method, high performance liquid chromatography and differential scanning calorimetry. *Analytica Chimica Acta* **650**, 227-233 (2009).
33. Andri, B. et al. Optimization and validation of a fast supercritical fluid chromatography method for the quantitative determination of vitamin D3 and its related impurities. *Journal of Chromatography A* **1491**, 171-181 (2017).
34. Sender, M. & Ziegenbalg, D. Light sources for photochemical processes - estimation of technological potentials. *Chemie Ingenieur Technik* **89**, 1159-1173 (2017).
35. Kneissl, M. et al. The emergence and prospects of deep-ultraviolet light-emitting diode technologies. *Nature Photonics* **13**, 233-244 (2019).
36. Muramoto, Y., Kimura, M. & Nouda, S. Development and future of ultraviolet light-emitting diodes: UV-LED will replace the UV lamp. *Semiconductor Science and Technology* **29**, 084004 (2014).